

An equation-free approach to coupled oscillator dynamics

Sung Joon Moon¹, R. Ghanem², and I. G. Kevrekidis^{1*}

¹*Department of Chemical Engineering & Program in Applied and Computational Mathematics (PACM), Princeton University, Princeton, NJ 08544, USA*

²*Department of Civil Engineering, University of Southern California, Los Angeles, CA 90089, USA*

(Dated: November 2, 2019)

We present an equation-free computational approach to the study of the coarse-grained dynamics of *finite* assemblies of *non-identical* coupled oscillators at- and near-synchronization. Using Wiener’s polynomial chaos coefficients as the coarse-grained observables, and exploiting short bursts of appropriately initialized detailed simulations, we circumvent the derivation of closures for the long-term dynamics of the assembly statistics.

PACS numbers: 05.45.Xt, 05.10.-a, 87.10.+e

Since Winfree’s pioneering work in 1960’s [1], coupled oscillator models have been investigated extensively. Some exact results on the collective dynamics for an infinite number of coupled oscillators (the so-called continuum-limit) [2, 3, 4] have shed light on synchronization phenomena in biological [1, 2, 5, 6, 7, 8], chemical [9, 10], and physical systems [11, 12] (see Ref. [13] for an excellent description). However, even in this ideal limit, some basic questions including global, quantitative stability of asymptotic states still remain open [14, 15, 16]. Many real-world systems consist of a large, *finite* number of non-identical entities, where statistical techniques for the continuum-limit are not directly applicable. Exploring and understanding the dynamics of such *finite* oscillator assemblies is an important topic (e.g. see Ref. [17]).

We present a computer-assisted approach to modeling the *coarse-grained* dynamics of such large, *finite* oscillator assemblies at- and near-synchronization. The premise is that a small number of coarse-grained variables (observables) of the oscillator assembly can adequately describe the long-term dynamics; alternatively, that a closed evolution equation for these observables exists, but is not explicitly available. To account for oscillator variability within the assembly, we treat both the variable oscillator properties (here, natural frequencies) and the oscillator states (here, phase angles) as random variables. The latter are expressed as a polynomial expansion of the former (borrowing Wiener’s polynomial chaos (PC) tools [18]); the PC expansion coefficients are our coarse observables.

Availability of the governing equations for the variables of interest is a prerequisite to modeling and computation. We circumvent this step using the recently-developed *equation-free* (EF) framework for complex, multiscale systems modeling [19, 20, 21]. In this framework we can perform system-level computational tasks without explicit knowledge of the coarse-grained equations; these unavailable equations are solved by designing, performing and processing the results of short bursts of appropriately initialized detailed (fine-scale, microscopic) simulations.

Our illustrative example is a paradigmatic model of

coupled oscillators, the Kuramoto model, consisting of a population of N all-to-all, phase-coupled limit-cycle oscillators with i.i.d. natural frequencies ω with distribution function $g(\omega)$ (of a small variance). This model has been extensively studied because of its simplicity and a certain mathematical tractability; yet it is not merely a toy model: It appears as a normal form for general systems of coupled oscillators (e.g. Refs. [10, 11]).

We choose a Gaussian $g(\omega)$ with variance $\sigma_\omega = 0.1$; however, our approach is not limited to this particular choice, nor to the Kuramoto model. Due to rotational symmetry, the mean frequency $\Omega = \sum_i \omega_i / N$ can be set to 0 without loss of generality. The governing equation for the phase angle of the i th oscillator θ_i is

$$\frac{d\theta_i}{dt} = \omega_i + \frac{K}{N} \sum_{j=1}^N \sin(\theta_j - \theta_i), \quad 1 \leq i \leq N, \quad (1)$$

where $K \geq 0$ is the coupling strength. This model exhibits spontaneous synchronization (phase-locking) at sufficiently large K . As K decreases across a critical value K_{tp} , more and more oscillators desynchronize until they all essentially evolve with their own frequencies below another critical value K_c [3, 14, 15]. In the continuum limit $N \rightarrow \infty$, Kuramoto [3] introduced a complex order parameter $re^{i\psi} = \frac{1}{N} \sum_{j=1}^N e^{i\theta_j}$ to describe the long-time states; the effective radius $r(t)$ measures the phase coherence, and $\psi(t)$ is the average phase angle. The asymptotic value of r ($t \rightarrow \infty$) in the continuum-limit exhibits a temporal analog of phase transition at K_c [3].

The order parameter r is a convenient representation of the asymptotic state in the continuum-limit; however, it does not uniquely specify the microscopic state, and it may not adequately describe transient dynamics during the approach to an asymptotic state. The statistical moments of the phase angle distribution function $\mathcal{M}_n \equiv \frac{1}{N} \sum_{j=1}^N \left(\theta_j - \frac{1}{N} \sum_{i=1}^N \theta_i \right)^n$, where n is a positive integer, are a “natural” first choice of coarse-grained observables (in a kinetic theory-like description). Because of symmetry we consider only even (nonvanishing) moments, and test whether a closure in terms of \mathcal{M}_2 and

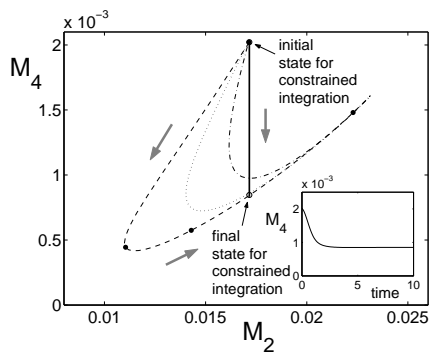


FIG. 1: Three *coarsely identical* (same \mathcal{M}_2 and \mathcal{M}_4) but microscopically different initializations (dashed, dotted and dot-dashed lines; see text) evolve along *different trajectories*, ultimately to the same slow manifold and synchronized state ($N = 300$; $K = 0.7 > K_{tp}$). Constraining the evolution to $\mathcal{M}_2 = 0.017$ (solid line) guides the trajectory directly to this slow manifold; the inset shows \mathcal{M}_4 becoming slaved to \mathcal{M}_2 during this constrained evolution by $t \approx 2.0$.

\mathcal{M}_4 is likely for $K > K_{tp}$. We prepare several distinct initial phase angle distributions with identical coarse-grained values ($\mathcal{M}_2 = 0.017$ and $\mathcal{M}_4 = 0.0020$); these phase angles are randomly assigned to oscillators, picked from $g(\omega)$. The phase portrait in Fig. 1 shows direct simulation [using Eq. (1)] for three of these initial assemblies; the trajectories are clearly distinct, suggesting that the dynamics cannot close simply on these two observables. Including higher order moments (such as \mathcal{M}_6) as observables does not remedy the situation. It is also clear, however, that the *long-term dynamics* lie on a low-dimensional manifold (ultimately a one-dimensional one) towards which all trajectories are eventually attracted.

The dynamical differences among the above three cases arise from the microscopic differences of the (macroscopically identical) initial conditions; this is best seen in the $\omega - \theta$ plane of Fig. 2. As all transients initially approach the slow manifold, *correlations* develop between individual phase angles and natural frequencies (the random initial “cloud” in the $\omega - \theta$ plane quickly evolves to a “curve”): The oscillators “sort themselves out”. These correlations were not accounted for when we randomly assigned angles to oscillators in the assembly.

We now include a “remedial initialization” step, evolving the dynamics by *constraining them* on prescribed values of the moments, as a system of differential algebraic equations (DAEs) using Lagrange multipliers. The solid line in Fig. 1 shows this preparatory step with a constraint on \mathcal{M}_2 only; constrained evolution brings the assembly down to the right point on the slow manifold, and the same “sorting” ($\omega - \theta$ correlation) develops as in the freely-evolving case. Phase angle statistics alone do not, therefore, constitute good observables [22]; correlations between natural frequencies and phase angles *must* be

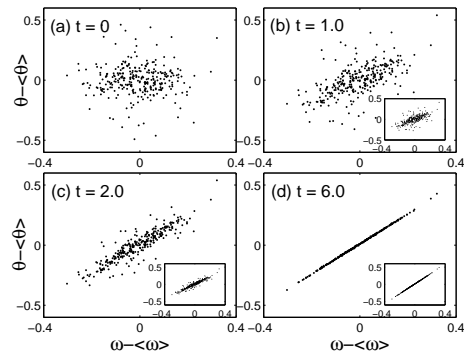


FIG. 2: Time snapshots in the $\theta - \omega$ plane for free evolution (main panels; dashed line in Fig. 1) and for constrained evolution (insets; solid line in Fig. 1) respectively. Each dot represents an oscillator, and (a) to (d) are snapshots at $t = 0, 1.0, 2.0$, and 6.0 , respectively, marked by filled circles in Fig. 1. Strong correlations develop during the initial transient stages (“oscillator sorting”).

included in the coarse description.

Motivated by this observation, we explore the long-term dynamics with a *different* set of observables, treating both θ and ω as random variables. The former is expanded in Hermite polynomials of the latter Gaussian random variable; Wiener’s polynomial chaos is the appropriate choice for Gaussian distributions. Generalized polynomial chaos (gPC) [23] would be invoked for different frequency distributions. For convenience, we introduce the normalized random variable $\xi = \omega/\sigma_\omega$. Our θ is expressed as

$$\theta(\omega, t) = \sum_{i=0}^p \alpha_i(t) H_i(\xi) = \sum_{i=0}^p \frac{\langle \theta, H_i \rangle}{\langle H_i, H_i \rangle} H_i(\xi), \quad (2)$$

where p is the highest order retained in the truncated series, $\langle \cdot, \cdot \rangle$ denotes the inner product w.r.t the Gaussian measure, and H_i is the i th Hermite polynomial [$H_0(x) = 1, H_1(x) = x, H_2(x) = x^2 - 1, H_3(x) = x^3 - 3x, \dots$]. Only odd-order α_i ’s are considered, due to symmetry. We will see that here the first two nonvanishing coefficients α_1 and α_3 provide an adequate representation. Given a particular detailed realization of the oscillator state, its PC coefficients α_i ’s are estimated through a least squares fitting algorithm, interpreting θ as an empirical function $f(\xi) \equiv \alpha_1 \xi + \alpha_3 (\xi^3 - 3\xi)$ and minimizing the residual $R^2 \equiv \sum_i [\theta_i - f(\xi_i; \alpha_1, \alpha_3)]^2$; ξ_i denotes a set of independent realizations of the random variable ξ . This procedure corresponds to the *restriction* (fine to coarse) step in the EF framework, described below.

In the EF approach, appropriately initialized short bursts of detailed, fine-scale simulation are used to estimate quantities pertaining to the evolution of the coarse-grained variables (observables). Lacking an explicit coarse-grained model in terms of the first few PC coefficients, we *estimate* the quantities necessary for scientific

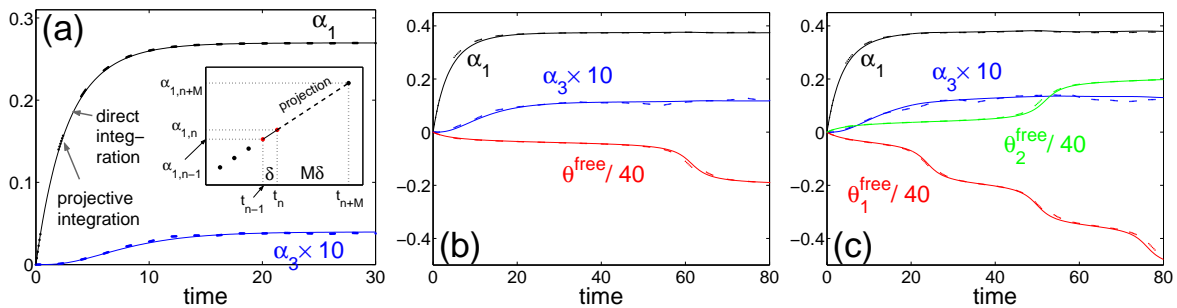


FIG. 3: (color online) Coarse projective integration (dots) and detailed coupled oscillator dynamics (lines); $N = 300$. (a) Two PC coefficients ($K = 0.4$; synchronization). (b) Two PC coefficients and a single “free” oscillator ($K = 0.31$). (c) Two PC coefficients and two “free” oscillators ($K = 0.31$). Natural frequencies are newly drawn from $g(\omega)$ at each lifting step (see text). Inset in (a): Schematic of a projective integration step: The last part (last two dots, at t_{n-1} and t_n) of a short burst of direct integration (five dots) is used to estimate the local time derivative (solid line). PC values at a future time $t = t_{n+M}$ are “projected” through forward Euler, i.e., $\alpha_1|_{t=t_{n+M}} = \alpha_1|_{t=t_n} + \frac{\alpha_{1,n} - \alpha_{1,n-1}}{t_n - t_{n-1}}(t_{n+M} - t_n)$.

computation with it (time derivatives, action of Jacobians, residuals) through *on demand* numerical experimentation with the detailed, fine-scale model [Eq. (1)].

The general procedure consists of (i) identifying good observables that sufficiently describe the coarse-grained dynamical state (here, a few α_i ’s), (ii) constructing a *lifting* operator, mapping the coarse description to one (or more, for variance reduction purposes) consistent fine-scale realization(s) [randomly drawing ω from $g(\omega)$ and assigning θ , using Eq. (2) and the given α_i values], (iii) evolving the lifted, fine-scale initial conditions for certain time horizon, (iv) *restricting* the resulting fine-scale description to the coarse observables [finding the PC coefficients of the final state] and (v) repeating the procedure as necessary to perform specific scientific computation steps. This is a general approach that has been combined with various fine-scale models (e.g. lattice-Boltzmann, kinetic Monte Carlo, molecular dynamics, Brownian dynamics) in many applications [19, 24]; see Ref. [20] for a review.

We first demonstrate *coarse projective integration* [25]. Each group of five dots in Fig. 3 represents the time horizon during which the detailed equations are integrated to enable the projective step; the local time derivative of the observables is estimated here simply from the last two dots in each group. Coarse variable values at a projected, future time are estimated using these derivatives and (for projective forward Euler) *linear* extrapolation in time [see the inset in Fig. 3 (a)]. Different continuum schemes lead to different projective integration algorithms (e.g. see Ref. [26]). After the projection step we *lift* the coarse variables to consistent fine-scale realizations, and use these as the initial condition for another short burst of direct detailed integration [step (iii) above]. Depending on the relative lengths of the projection step and the short run required to estimate the coarse time derivatives, this procedure may significantly accelerate

the computational evolution of the oscillator *statistics*; the cost of the lifting step (here negligible) must also be considered. At each lifting step, ω was *newly* drawn from $g(\omega)$, and the full integration (lines) and projective integration (dots) agree on the level of fluctuation among realizations. The PC coefficients display smooth behavior, nearly independently of particular random draws; for the *same* random draw at every step results would be even better. Projective integration in Fig. 3 (a) required in our illustration reduced the direct integration computational effort by a factor of four. Efficiency and accuracy (also estimation issues) for (coarse) projective integration are discussed elsewhere (e.g. Ref. [26]); here we simply demonstrated the procedure and its potential.

Direct, long-time simulation is often inefficient in computing long-time (stationary) states, and their stability and parametric dependence; equation-free *fixed-point algorithms* can instead be used to compute the PC coefficients of such final, synchronized stationary states. Starting from an initial condition $\alpha \equiv (\alpha_1, \alpha_3)^T$ we lift, and integrate the full model for time ΔT . We then restrict to the observables of the final state $\Phi_{\Delta T}$; this is the *coarse timestepper*. We now solve for the fixed point satisfying $\Phi_{\Delta T}(\alpha) - \alpha = 0$, through a (coarse-grained) Newton-Raphson method [20]; the residual and the action of the unavailable Jacobian are numerically estimated through short bursts of direct detailed simulations, appropriately initialized at *coarsely nearby* initial conditions. The iteration converges nearly quadratically down to the level of fluctuations (see Tab. I); matrix-free iterative methods (e.g. Newton-GMRES [27]) also converge in a few steps. Both stable *and unstable* coarse steady states can be found this way. Fluctuations of the PC coefficients were generally two orders of magnitude smaller than those of \mathcal{M}_n ’s (as the latter are dominated by the oscillators in the distribution tail); relatively small realization ensembles were sufficient for variance reduction.

TABLE I: Steady state value computation of α_1 and α_3 at $K = 0.5$ for $N = 300$, using coarse Newton-Raphson. Values at each iteration have been averaged over an ensemble of 100 realizations.

iteration	α_1	α_3	$ \Delta\alpha_1 + \Delta\alpha_3 $
0	3.0000×10^{-1}	1.0000×10^{-2}	1.1273×10^{-1}
1	1.9895×10^{-1}	-1.6763×10^{-3}	1.3261×10^{-2}
2	2.0895×10^{-1}	1.5813×10^{-3}	1.7710×10^{-4}
3	2.0907×10^{-1}	1.6404×10^{-3}	6.8305×10^{-6}
4	2.0906×10^{-1}	1.6380×10^{-3}	

Slightly below the transition value K_{tp} , where only few oscillators become desynchronized, it makes sense to consider the system as a combination of synchronized “bulk” and a few “free” oscillators. Good coarse-grained observables then are a few PC coefficients for the “bulk” synchronized oscillators and the phase angle(s) of the (few) desynchronized one(s). The EF approach can be directly “wrapped around” this alternative representation. Both for the one free and two free oscillator cases, projective integration on the new observables successfully track (and accelerate) direct detailed simulation [Figs. 3 (b) and (c)]. These “good observables” are suggested by direct inspection and common sense; for more complicated, high-dimensional problems, good state parameterizations require modern data mining algorithms. Diffusion maps on graphs constructed by the data [28] are a promising tool for detecting good “reduction coordinates” (observables) on which to base EF computations.

In summary, the EF multiscale approach was successfully used for coarse-grained dynamic computations of finite assemblies of non-identical coupled oscillators; the derivation of explicit closures at- and close to the synchronized regime was circumvented. Initial transient “sorting” of the oscillators, establishing correlations between natural frequencies and phase angles, suggested Wiener PC coefficients as the appropriate coarse observables. If the problem dynamics can be coarse-grained and if good coarse observables are known, traditional numerical analysis algorithms can be used as protocols for the “intelligent” design of short bursts of computational experiments with the detailed, fine-scale model. The approach can be directly generalized to accelerate the simulation and modeling of more complicated oscillator dynamics, more diverse natural frequency distributions (e.g. bimodal) and more general coupling topologies.

This work was supported by DARPA and by the National Science Foundation.

* yannis@arnold.princeton.edu

[1] A. T. Winfree, *J. Theor. Biol.* **16**, 15 (1967).

- [2] Y. Kuramoto, *Chemical Oscillations, Waves, and Turbulence*, Springer-Verlag (1984).
- [3] Y. Kuramoto, in *International Symposium on Mathematical Problems in Theoretical Physics*, Edited by H. Arakai, Lecture Notes in Physics, Vol. 39, (Springer, New York, 1975), p. 420.
- [4] J. T. Ariaratnam and S. H. Strogatz, *Phys. Rev. Lett.* **86**, 4278 (2001).
- [5] C. M. Gray, P. Konig, A. K. Engel, and W. Singer, *Nature* **338**, 334 (1989).
- [6] J. Buck, *Quart. Rev. Biol.* **63**, 265 (1988).
- [7] T. J. Walker, *Science* **166**, 891 (1969).
- [8] Z. Néda, E. Ravasz, Y. Brechet, T. Vicsek, and A. L. Barabási, *Nature* **403**, 849 (2000).
- [9] G. Ertl, *Science* **254**, 1750 (1991).
- [10] I. Z. Kiss, Y. Zhai, and J. L. Hudson, *Science* **296**, 1676 (2002).
- [11] K. Wiesenfeld, P. Colet, and S. H. Strogatz, *Phys. Rev. Lett.* **76**, 404 (1996).
- [12] R. A. Oliva and S. H. Strogatz, *Int. J. Bifurcation Chaos* **11**, 2359 (2001).
- [13] S. H. Strogatz, *SYNC: the Emerging Science of Spontaneous Order*, Hyperion, New York (2003).
- [14] S. Strogatz, *Physica D* **143**, 1 (2000).
- [15] S. C. Manrubia, A. S. Mikhailov, and D. H. Zanette, *Emergence of Dynamical Order*, World Scientific, Singapore (2004).
- [16] J. A. Acebrón, L. L. Bonilla, C. J. Pérez Vicente, F. Ritort, and R. Spigler, *Rev. Mod. Phys.* **77**, 137 (2005).
- [17] N. J. Balmforth and S. Sasi, *Physica D* **143**, 21 (2000).
- [18] R. Ghanem and P. Spanos, *Stochastic Finite Elements: A Spectral Approach*, Springer-Verlag, New York (1991).
- [19] C. Theodoropoulos, Y. H. Qian, and I. G. Kevrekidis, *Proc. Natl. Acad. Sci. USA* **97**, 9840 (2000).
- [20] I. G. Kevrekidis *et. al*, *Comm. Math. Sciences* **1** (4), 715 (2003); e-print physics/0209043.
- [21] I. G. Kevrekidis, C. W. Gear, and G. Hummer, *AICHe J.*, **50**, 1346 (2004).
- [22] S. J. Moon and I. G. Kevrekidis, “An equation-free approach to coupled oscillator dynamics”, *Int. J. Bifur. Chaos*, in press (2005); e-print nlin.AO/0502016.
- [23] D. Xiu and G. Em Karniadakis, *SIAM J. Sci. Comput.* **24**, 619 (2002).
- [24] C. W. Gear, I. G. Kevrekidis, and C. Theodoropoulos, *Chem. Eng.* **26**, 941 (2002); A. G. Makeev, D. Maroudas, A. Z. Panagiotopoulos, and I. G. Kevrekidis, *J. Chem. Phys.* **117**, 8229 (2002); C. Siettos, M. D. Graham, and I. G. Kevrekidis, *J. Chem. Phys.* **118**, 10149 (2003); G. Hummer and I. G. Kevrekidis, *J. Chem. Phys.* **118**, 10762 (2003).
- [25] C. W. Gear and I. G. Kevrekidis, *SIAM J. Sci. Comput.* **24**, 1091 (2003).
- [26] R. Rico-Martinez, C. W. Gear, and I. G. Kevrekidis. *J. Comp. Phys.*, **196**, 474 (2004).
- [27] C. T. Kelley, *Iterative Methods for Linear and Nonlinear Equations (Frontiers in Applied Mathematics, Vol. 16)*, SIAM, Philadelphia (1995).
- [28] B. Nadler, S. Lafon, R. C. Coifman, and I. G. Kevrekidis, “Diffusion Maps, Spectral Clustering and the Reaction Coordinates of Dynamical Systems”, *Appl. Comp. Harm. Anal.*, in press; e-print math/0503445.